Melanoma Cells Express Elevated Levels of Phosphorylated Histone H2AX Foci

Raymond L. Warters,* Patrick J. Adamson,* Christopher D. Pond,* and Sancy A. Leachman†
Departments of *Radiation Oncology and †Dermatology, University of Utah Health Sciences Center, Salt Lake City, Utah, USA

When human cells sustain a DNA double-strand break (dsb), histone H2AX in chromatin surrounding the DNA break is phosphorylated, marking repair foci. The number of phosphorylated histone H2AX (γH2AX) foci approximates the number of dsb present in the cell's nuclear DNA. We observed 0.4 γH2AX foci per nucleus in primary human melanocytes. In contrast, in four melanoma cell lines, we detected 7–17 γH2AX foci per nucleus, a 17–42 times increase in the basal level of γH2AX foci in melanoma cells relative to melanocytes (MC). Thus, untreated melanoma cells express significantly greater numbers of γH2AX foci than do untreated MC. Detection and rejoining of ionizing radiation-induced DNA dsb proceeded as rapidly in melanoma cells as in MC. Melanoma cells, however, reduced the number of radiation-induced γH2AX foci down only to pre-irradiation levels. Co-localization of the majority of γH2AX foci with ataxia telangiectasia mutated, BRCA1, 53BP1, and Nbs1 foci in untreated melanoma cells indicated that the additional foci in melanoma cells were associated with a DNA change that the cells interpret as DNA dsb. Co-localization of γH2AX foci with the telomere replication factor 1 protein in untreated melanoma cells indicates that the additional foci in untreated melanoma cells are associated with dysfunctional telomeres that induce a DNA damage stress response.

Key words: chromosome instability/γH2AX foci/melanocyte/micronuclei/telomere dysfunction
J Invest Dermatol 124:807–817, 2005

The skin is the primary barrier for humans against the external environment. Thus, skin cells are frequently the first cells to be exposed to physical and chemical genotoxic agents such as ultraviolet (UV) and ionizing radiations (IR). Exposure to UV radiation is considered to be the major contributing factor to melanomagenesis (Jhappan *et al*, 2003), although the molecular pathway(s) leading from UV-induced DNA photoproducts to melanoma is as yet unclear. Melanoma develops through well-defined morphological and histological stages that involve the loss of control of cell proliferation, acquisition of invasiveness, and ultimately acquisition of metastatic potential (Clark *et al*, 1984). The normal melanocytic cell, presumably damaged in its genome by sun exposure, develops through primary melanoma *in situ* and ultimately to metastatic melanoma. From its earliest stages, melanomagenesis involves elevated frequencies of mutations and/or loss of tumor suppressors and oncogenes (Albino *et al*, 1997; Hussein and Wood, 2002), microsatellite instability (Hussein and Wood, 2002), aneuploidy detected with increases in the DNA content (Pilch *et al*, 2000; Runger *et al*, 2003), and an increase in the frequency of micronuclei (Runger *et al*, 2003).

The chromosome rearrangements observed in melanoma cells likely require naturally or environmentally induced DNA double-strand breaks (dsb) as intermediates. The presence of DNA dsb in the cell genome induces formation of repair foci (Petrini and Stracker, 2003). So one approach to assess the involvement of DNA dsb in chromosome instability is to evaluate the expression of dsb-induced repair foci in melanoma cells. Nuclear phosphatidylinositol 3–OH serine/threonine protein kinase-like kinases (PIKK) recognize the presence of DNA dsb in the cell DNA, and transduce this fact via phosphorylations to downstream effector proteins that participate in DNA dsb repair processes. One type of DNA dsb repair focus involves phosphorylated H2AX (γH2AX) histone proteins (Sedelnikova *et al*, 2002; Rothkamm and Lobrich, 2003). Production of DNA dsb in nuclear DNA induces phosphorylation of the H2AX histone at serine 139, which is in an evolutionarily conserved PIKK motif (Rogakou *et al*, 1998, 2000; Burma *et al*, 2001). Two nuclear PIKK, the ataxia telangiectasia mutated (ATM) and DNA-dependent protein kinase (DNA PK) protein kinases, have been shown to phosphorylate histone H2AX in response to IR forming nuclear foci (Burma *et al*, 2001; Bakkenist and Kastan, 2003; Park *et al*, 2003; Stiff *et al*, 2004). As the ATM and DNA PK kinases phosphorylate the H2AX protein in chromatin adjacent to a DNA dsb, the locally high concentration of γH2AX protein can be detected by immunofluorescence as foci (Rogakou *et al*, 1999; Rothkamm and Lobrich, 2003). In addition to trauma-induced DNA dsb, phosphorylated H2AX histone foci have been detected in S-phase cells (Mirzoeva and Petrini, 2003) and at uncapped telomeres (Takai *et al*, 2003). There is a close correlation between the number of DNA dsb and the

Abbreviations: ATM, ataxia telangiectasia mutated; DI, DNA index; DNA PK, DNA-dependent protein kinase; dsb, double-strand break; FB, fibroblasts; IR, ionizing radiation; PBS, phosphate-buffered saline; PIKK, protein kinase-like kinases; MC, melanocytes; TRF, telomere replication factor

Copyright © 2005 by The Society for Investigative Dermatology, Inc.

number of Type II nuclear γH2AX foci induced by IR (Sedelnikova *et al*, 2002; Rothkamm and Lobrich, 2003). Therefore, the number of γH2AX foci has been taken to indicate the number of DNA dsb in the cell's nuclear DNA (Sedelnikova *et al*, 2002; Rothkamm and Lobrich, 2003).

In a recent study of the expression of phosphorylated H2AX histone in cultured primary skin cells and their cancers, we found that untreated cancer cells expressed significantly higher levels of γH2AX foci than did primary skin cells. These phenomenological observations suggested that some characteristics of skin cancer cells result in higher basal levels of DNA repair foci. As some chromosome rearrangements require DNA dsb as an intermediate, and melanoma cells generally express chromosome instability during their development, we speculated that the high basal levels of γH2AX foci might reflect high levels of chromosome instability in these cancer cells. In this report we have examined the relationship between the expression of DNA γH2AX foci and the expression of chromosome instability (i.e., micronuclei) in melanocytes (MC) and melanoma cells.

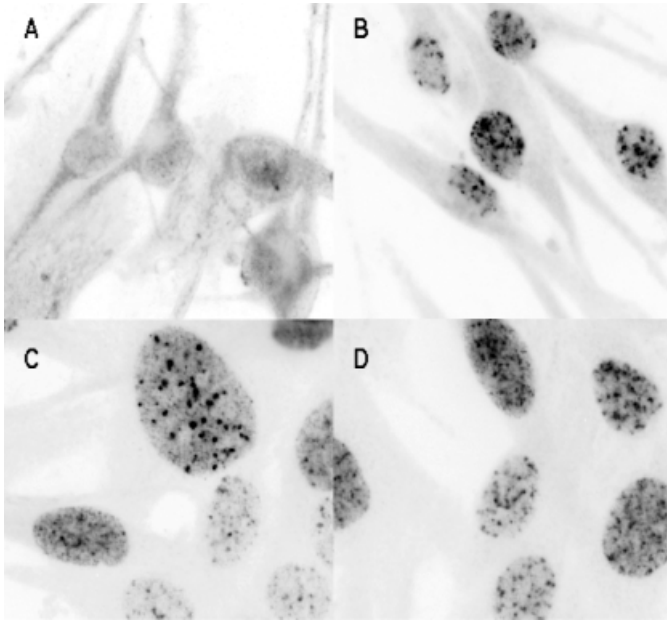

Figure 1
Detection of γH2AX foci in primary melanocytes (MC) and melanoma cells. Primary neonatal MC (*Panels A* and *B*) or YUSAC2 melanoma cells (*Panels C* and *D*) were grown on serum-coated cover slips and either exposed to 1.5 Gy of γ radiation (*Panels B* and *D*) or left unirradiated (*Panels A* and *C*). Cover slips were collected 60 min after treatment, the cells were fixed with formaldehyde, and analyzed for the presence of γH2AX in their nuclei by indirect immunofluorescence, as described above.

Results

Phosphorylated H2AX histone foci are detected in untreated MC and melanoma cells We recently examined cultured primary MC and melanoma cells by indirect immunofluorescence for the expression of γH2AX foci. γH2AX foci with a diameter of 0.25–1.0 μm were observed. The number of γH2AX foci observed in untreated MC was low (Fig 1*A*). The distribution of foci counted per nucleus in untreated MC was skewed toward cells containing less than 5 foci per nucleus. Ninety percent of MC contained 1 or no foci (Fig 2*A*). On an average 0.4, 0.8, and 2.0 γH2AX foci were detected per nucleus in untreated MC, fibroblasts (FB), and keratinocytes, respectively (Table I). This is within the range of values, from 0.05 to 1.5 foci per nucleus, reported in the literature for primary human FB (Rogakou *et al*, 1999; Rothkamm and Lobrich, 2003). In contrast, greater numbers of γH2AX foci were detected in the nuclei of untreated melanoma and carcinoma cells (Fig 1*C* and Table I). The distribution of γH2AX foci counted per untreated YUSAC2 nucleus was skewed toward 15–25 foci per nucleus (Fig 2*A*) with an average of 17 foci per cell nucleus (Table I). A shift toward higher numbers of foci/nucleus was also observed in the other melanomas examined (Fig 2*C*). Seventy-five percent of YUSIT1 cells contained 3 or more foci, whereas 76% of YUSAC2 cells contained 6 or more foci per nucleus. Detecting larger numbers of γH2AX foci in melanoma cells was not surprising because cancer cells have been reported to express higher numbers of γH2AX foci. For instance, about 2.5 foci per nucleus were reported to occur in a human astrocytoma and a fibrosarcoma (Rogakou *et al*, 1999; Sedelnikova *et al*, 2002). A range of γH2AX foci yields was also observed in untreated cells from other cancers. For instance, we observe 5.2 foci per HeLa S3 cell nucleus and 13.7 foci per HaCat cell nucleus (Table I). Our results indicated that untreated melanoma and carcinoma cells contain significantly higher numbers of γH2AX foci, and thus presumably DNA dsb, than do untreated primary MC.

DNA dsb detection in MC and melanoma cells A direct relationship between the number of DNA dsb induced by IR and the number of γH2AX foci has been reported (Sedelnikova *et al*, 2002; Rothkamm and Lobrich, 2003), indicating that the number of γH2AX foci detected in cell nuclei reflects the number of DNA dsb. When the length of double-stranded DNA prepared from untreated MC, YUSIT1, or YUSAC2 cells was compared on the type of pulsed field agarose gels that resolve *Schizosaccharomyces pombe* chromosomal DNA (Warters, 1992; Warters and Lyons, 1992), no consistent difference was detected between any of the three cell types (results not shown). But as the number of DNA dsb expected in melanoma cell DNA (i.e., about 17–20) is comparable to a radiation dose of about 0.5 Gy, and as this dose is below the resolution of this agarose gel approach (Warters and Lyons, 1992; Rothkamm and Lobrich, 2003), it is not surprising that we could not detect higher numbers of dsb in the melanoma cells than in MC by physical chemical methods.

To demonstrate that in our hands the γH2AX immunofluorescence approach actually detects DNA dsb, we compared the expression of γH2AX foci at various times after cells were exposed either to H_2O_2 or to γ radiation. H_2O_2 produces few DNA dsb. In contrast, IR is an efficient inducer of DNA dsb. Few additional γH2AX foci were induced over the background level for up to 4 h after cells were exposed to 20 μM H_2O_2 for 15 min at 4°C (results not shown). Significantly greater numbers of foci were detected when MC (Fig 1*B*) or YUSAC2 cells (Fig 1*D*) were collected and analyzed at various times after irradiation. The number of γH2AX foci expressed, as a function of time after

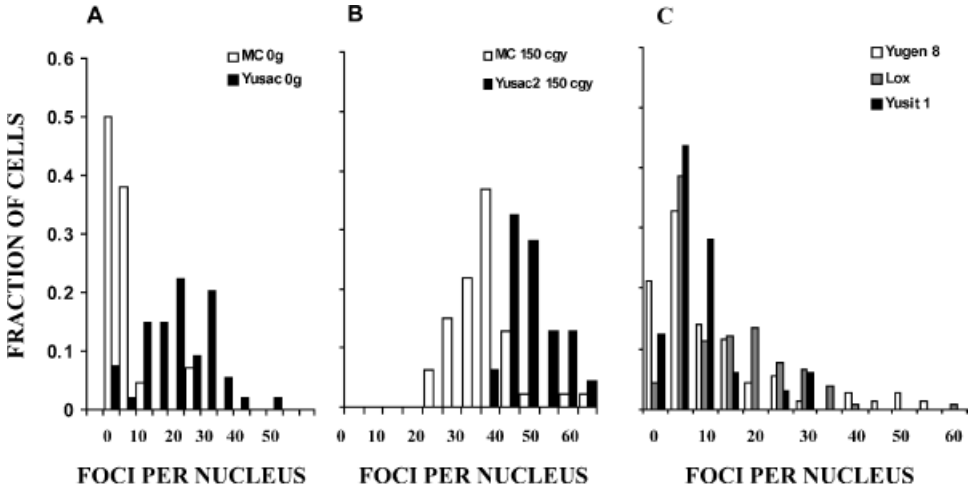

Figure 2
Distribution of γH2AX foci in untreated or irradiated melanocytes (MC) and YUSAC2 cells. MC (*open bars*) or YUSAC2 (*closed bars*) cells growing on serum-coated cover slips were left untreated (*Panel A*) or exposed to 1.5 Gy ionizing radiation (*Panel B*), collected at 60 min, and stained with an antibody against the γH2AX protein. Alternatively, untreated YUGEN8, LOX, and YUSIT1 cells were similarly collected and stained (*Panel C*). Cells were imaged by immunofluorescence microscopy and the number of γH2AX foci in more than 40 total cells per group counted. The fraction of cells counted that express the indicated numbers of repair foci is plotted.

irradiation, should indicate the efficiency at which MC or YUSAC2 cells recognize and respond to DNA dsb, and the efficiency with which those DNA dsb are rejoined (Rothkamm and Lobrich, 2003). As shown in Fig 3*A*, the number of γH2AX foci detected as a function of incubation time after exposure to 1.5 Gy increased to a maximum by 30–60 min, declined between 1 and 6 h with a half-time of about 3–4 h, and became essentially constant in both cell types by 8–12 h. There were two major differences in expression of γH2AX foci between the two cell types. The basal number of nuclear foci began at a higher number in YUSAC2 cells than in MC, and the number of residual γH2AX foci 12 h after irradiation approached the pretreatment number of foci in YUSAC2 cells, not the lower number observed in MC (Fig 3*A*). Sixty minutes after exposure to 1.5 Gy, the number of IR-induced foci redistributed to 25–30 in MC and 45–50 in YUSAC2 cells (Fig 2*B*). The total number of repair foci induced per Gy of IR (total nuclear foci in irradiated minus untreated cells) at all radiation doses was the same, or less, in YUSAC2 cells than in MC (Fig 3*B*). IR induced 21 and 16 foci per nucleus per Gy, respectively, in MC and YUSAC2 cells (Table I). This is about half the yield of foci or DNA dsb reported previously to occur in irradiated cells (Rothkamm and Lobrich, 2003). Our results indicate that whereas we may underestimate the number of foci in untreated or irradiated cells, expression of γH2AX foci detects IR-induced DNA dsb. The efficiency at which MC and YUSAC2 cells detect IR-induced DNA dsb and phosphorylate the H2AX

Table I. Yield of radiation-induced γH2AX foci

	γH2AX foci/nucleus[a]					
	0 Gy	1 Gy	Net change	Fraction S[b]	MN/1000 cells[c]	DI[d]
MC	0.4 ± 1.5	21 ± 6	20	0.23	9	1.0
FB	0.8 ± 1.9	27 ± 10	26	0.15	15	1.1
KC	2.0 ± 3.5	31 ± 9	29	ND	45	ND
HeLa	5.2 ± 4.4	ND	ND	0.41	179	1.6
YUSIT	6.5 ± 7.3	32 ± 12	26	0.26	478	1.8
YUGEN	10 ± 13	33 ± 13	24	0.41	476	1.7
LOX	11 ± 11	28 ± 11	18	0.40	32	1.6
HaCaT	14 ± 10	ND	ND	0.47	57	1.5
YUSAC	17 ± 412	32 ± 8	16	0.43	218	1.7

[a]Proliferating primary melanocytes (MC), fibroblasts (FB), or keratinocytes (KC); YUSIT1, YUSAC2, YUGEN8, or LOX melanoma cells, and HeLa or HaCaT carcinoma cells growing on glass cover slips, were exposed to 1 Gy of γ rays, or left untreated, and collected at 60 min. The cells were fixed with formaldehyde 60 min after treatment, exposed to a primary antibody to γH2AX and subsequently to a secondary antibody conjugated to the Alexa 488 fluorescent dye.Images (similar to Fig 1) were quantified using a fluorescence microscope and the results in one representative experiment out of at least two repeat experiments are expressed as the total number of γH2AX foci detected per nucleus (average ± 1 SD). The net change is the total number of foci in irradiated minus the total number of foci in untreated cells.
[b]The average fraction of untreated cells found to be in the S phase of the cell cycle in two to four repeats was determined by flow cytometry.
[c]Untreated cells were exposed to 3 μg per mL Cytochalasin B for 48 h. Cells on coverslips were collected, stained with diamidinophenyl indole and the number of micronuclei in ⩾1000 total binucleated cells determined. Data are expressed as the total number of micronuclei per 1000 binucleated cells.
[d]The untreated cell DNA index (DI) is expressed as the ratio of the G_1 DNA content in test cells/the G_1 DNA content in MC, as described in the Materials and Methods section.
ND, not determined.

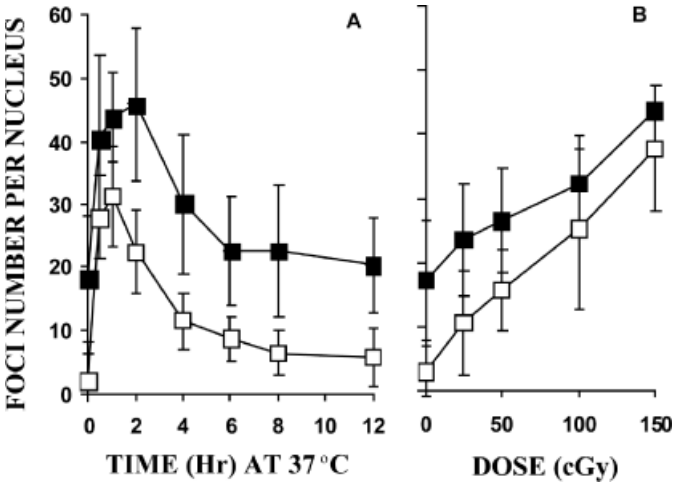

Figure 3
Expression of γH2AX repair foci in irradiated melanocytes (MC). (*Panel A*) Appearance and disappearance of ionizing radiation- (IR-) induced γH2AX foci in MC and YUSAC2 cells. MC (open symbols) or YUSAC2 cells (closed symbols) were exposed to 1.5 Gy of γ irradiation, replaced at 37°C, and collected at increasing times, as indicated. The number of γH2AX foci per cell nucleus was quantified at each time point and plotted (Av ± 1 SD). (*Panel B*) Concentration dependence for the expression of IR induced repair foci. MC or YUSAC2 cells were exposed to increasing γ ray doses, replaced at 37°C for 60 min, and the number of γH2AX foci/nucleus quantified as described above.

protein, the expression kinetics of repair foci as a function of time after exposure to IR, and the residual number of foci remaining in cell nuclei 12 h after irradiation are the same in both cell types. Thus, both MC and YUSAC2 cells recognize IR-induced DNA dsb and articulate this into repair foci with similar efficiencies.

γH2AX foci in untreated cells co-localize with DNA repair complex proteins Our results (Fig 3*B* and Table I) indicate that in all irradiated cells, PIKK, such as the ATM protein, recognize IR-induced DNA dsb, are activated, and phosphorylate the H2AX histone to an equivalent extent. As the number of foci remaining in previously irradiated YUSAC2 cells is the same as the number of foci that existed prior to irradiation (Fig 3*A*), the repair process that rejoins IR-induced DNA dsb appears not to act on the DNA changes that existed prior to irradiation. Thus, this pre-existing DNA damage must be qualitatively different from IR-induced DNA dsb. To examine the similarity of this pre-existing DNA damage with IR-induced dsb, untreated or irradiated cells were exposed simultaneously to antibodies against γH2AX and other proteins that localize to induced DNA dsb. Antibodies to the ATM protein phosphorylated on serine 1981, to 53BP1 protein phosphorylated on serine 25 and to the BRCA1 protein formed foci in irradiated, as well as untreated, melanoma cells, and co-localized with γH2AX foci. Approximately 80%–90% of γH2AX foci co-localized with either the 53BP1, the BRCA1, or the phosphorylated ATM protein foci observed in untreated, as well as in irradiated, primary and melanoma cells (Fig 4). As the BRCA1 and phosphorylated form of the 53BP1 protein forms foci at DNA dsb (Celeste *et al*, 2003), these results are consistent with the γH2AX foci detected in melanoma cells being associated either with DNA dsb or with some change in nuclear chromatin that is recognized as a DNA dsb.

Foci of the Nbs1 protein were formed, and co-localized with γH2AX foci, in MC and melanoma cells that were exposed to 100 cGy and collected 1 h after irradiation (results not shown). The Nbs1 also formed foci in untreated MC or melanoma cells (Fig 4). Approximately 80%–90% of the γH2AX foci observed in untreated YUSIT1 or YUSAC2 cells co-localized with Nbs1 protein foci. As the Nbs1 protein associates into multi-protein repair complexes at DNA dsb (Furuta *et al*, 2003), the results indicate that the γH2AX foci detected in untreated melanoma cells are present at chromatin sites and are associated with active DNA dsb repair complexes.

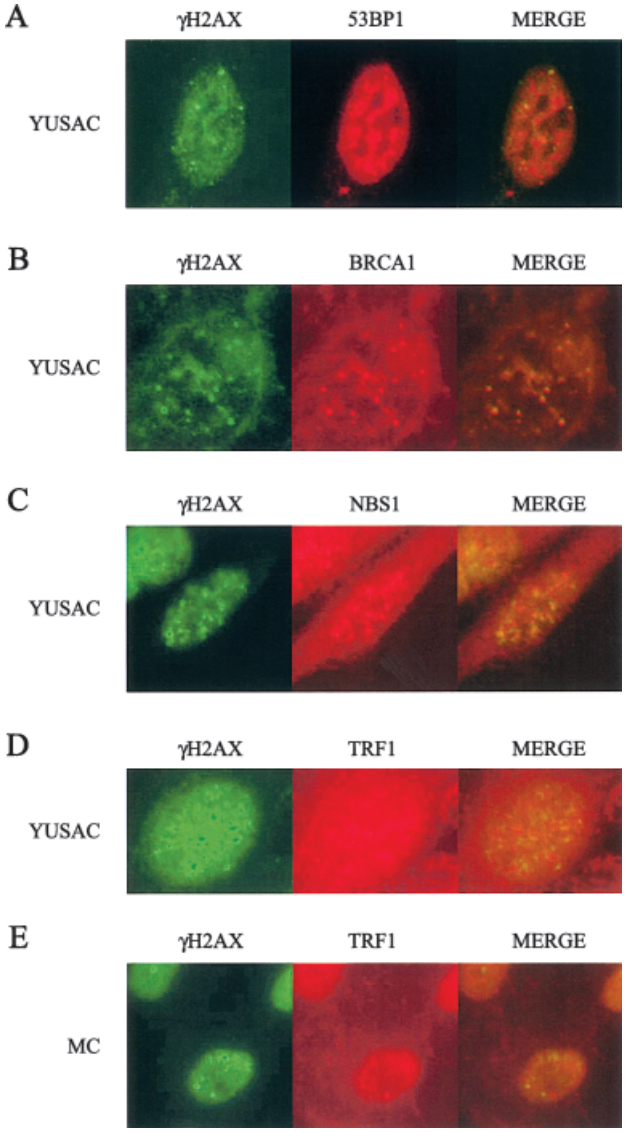

Figure 4
γH2AX foci co-localize with other double-strand break-associated proteins in untreated melanoma cells Untreated YUSAC2 (*Panels A–D*) or melanocytes (MC) (*Panel E*) were collected and exposed to primary antibodies against γH2AX and either 53BP1 (*Panel A*), BRCA1 (*Panel B*), Nbs1 (*Panel C*), or telomere replication factor 1 (TRF1) (*Panels D* and *E*). Cells were exposed to an Alexa 488-conjugated secondary antibody (green fluorescence) to γH2AX and an Alexa 568-conjugated secondary antibody to all other primary antibodies. Cells were imaged with a fluorescence microscope as described in Methods. Results very similar to YUSAC2 cells were obtained with YUSIT1 cells.

Untreated melanoma cells contain few apoptotic cells One possible explanation for the elevated numbers of γH2AX foci observed in untreated melanoma cells might be that there is a high basal level of apoptosis in melanoma cells. The magnitude of sub-diploid DNA in untreated MC, LOX, YUSIT, YUGEN, and YUSAC cells, determined by flow cytometry was 2.6%, 1.0%, 2.0%, 2.3%, and 4.3%, respectively, of the total cell population. Only YUSAC2 melanoma cells contained a sub-diploid DNA content greater than MC. Thus, melanoma cells contain low basal levels of apoptotic cells. Less than 1% of the cells in any of the melanomas had a nuclear morphology (i.e., perinuclear condensed chromatin or fragmented nuclei) consistent with cells that are in the process of apoptosis (Wyllie *et al*, 1980). Thus, the fraction of apoptosing melanoma cells is probably too small to significantly alter the number of foci counted in untreated melanoma cell lines. To further reduce this possibility, cells with abnormal nuclear morphologies were excluded from our results.

Cell cycle analysis Greater H2AX histone protein phosphorylation has been reported in the S phase of the cell cycle of untreated cells (Furuta *et al*, 2003; MacPhail *et al*, 2003; Mirzoeva and Petrini, 2003). Thus, another explanation for the higher frequency of foci in melanoma cells might be that cancer cells contain a higher fraction of proliferating cells and thus a higher fraction of S-phase cells than do MC. When the fraction of cells in the S phase of the cell cycle was determined by flow cytometry (Table I), increases in γH2AX foci generally correlated with increases in the fraction of S-phase cells. But whereas 30%–40% of melanoma cells are in the S phase of the cell cycle, the majority of melanoma cells (70%–80%) contain elevated levels of H2AX foci. Thus, it is unlikely that all γH2AX foci occur in S-phase cells.

To examine γH2AX expression throughout the cell cycle, untreated MC and melanoma cells were stained with propidium iodide for DNA content and with an antibody for phosphorylated H2AX, and analyzed by flow cytometry (Fig 5). All cell types examined, including MC, FB, YUSIT1, YUSAC2, and HaCaT, gave a qualitatively similar distribution of γH2AX fluorescence throughout the cell cycle. All cell cycle phases in all cells examined expressed at least some fluorescence, with total fluorescence in S and G_2\M phases being approximately two to three times greater than in G_1-phase cells. Total fluorescence throughout the cell cycle of YUSIT1 cells (Fig 5), as well as YUSAC2 cells (results not shown), was approximately 4–5-fold greater than observed in similar cell-cycle phases of MC. Thus, higher fractions of S phase and proliferating cells in melanomas cannot explain fully the increase in γH2AX foci in melanomas.

γH2AX foci co-localize with a telomere-associated protein in untreated melanoma cells A possible explanation for the elevated γH2AX foci in untreated melanoma cells might be that these cancer cells have aberrant telomere replication and/or aberrant telomere structure (Fagogna *et al*, 2003; Takai *et al*, 2003). To examine this possibility, we examined MC and melanoma cells for expression of γH2AX and telomere replication factor 1 (TRF1) (Fig 4). The TRF1 protein decorates nuclear telomeric DNA sequences and can be detected as foci in interphase cells (Chong *et al*, 1995; Shen *et al*, 1997). A large number of TRF1 foci, about 30–50, appeared to be present in MC, FB, and melanoma cells, but were too numerous to count (Fig 4). Additionally, there was about 1.5 to two times more TRF1 protein fluorescence from melanomas than from primary skin cells. Approximately, 50% of γH2AX foci in untreated MC and FB co-localized with TRF1 foci, whereas 60% or more of the γH2AX foci in untreated YUSIT1 or YUSAC2 cells co-localized with TRF1 foci (Fig 4). Thus, the majority of γH2AX foci observed in untreated MC or melanoma cells co-localize with foci of the TRF1 protein and thus likely co-localize with telomeric DNA sequences.

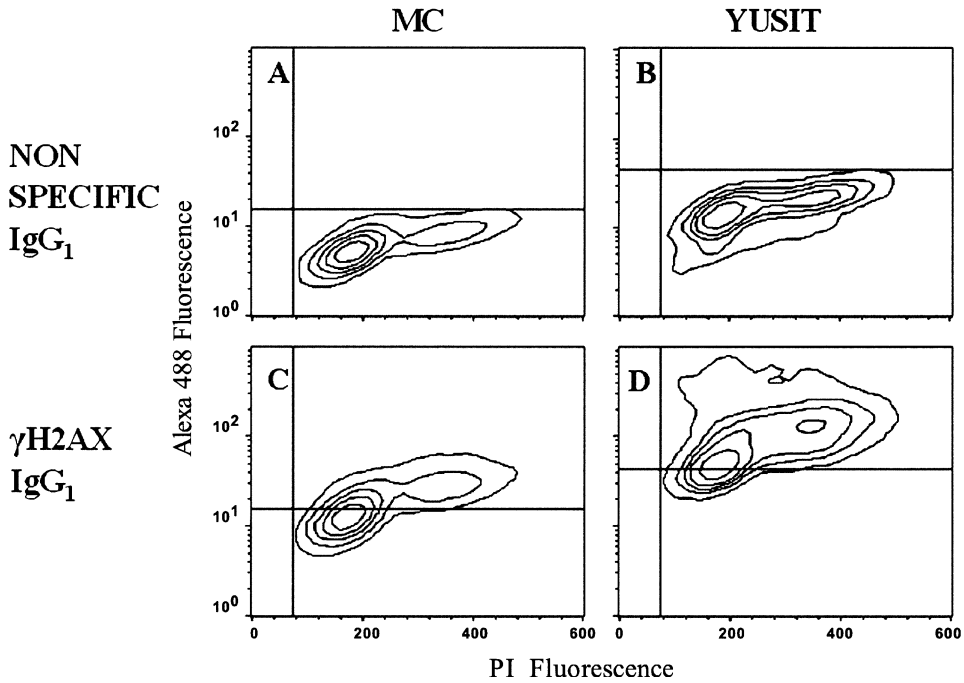

Figure 5
Flow cytometric analysis of γH2AX fluorescence throughout the cell cycle of melanocytes (MC) and YUSIT1 cells. MC (*Panels A* and *C*) or YUSIT1 cells (*Panels B* and *D*) were exposed either to a nonspecific immunoglobulin G_1 (IgG_1) protein (*Panels A* and *B*) or with the anti-γH2AX monoclonal antibody (*Panels B* and *D*). The cells were stained with an Alexa 488-conjugated, anti-mouse secondary antibody, their DNA stained with propidium iodide, and the cells analyzed by flow cytometry as described in Methods. The x-axis in arbitrary units represents increasing red (PI) fluorescence, the y-axis in arbitrary units represents increasing green (Alexa 488) fluorescence, and the z-axis represents the number of events (number of cells analyzed). Results are a representative experiment from two or more repeats. G_1 cells (at left of each panel) express lower red and green fluorescence relative to S and G_2/M cells.

Melanoma cells contain greater numbers of micronuclei Another approach to evaluate the number of DNA dsb occurring in untreated melanoma cells is to determine the occurrence of micronuclei in these cells. Micronuclei result from acentric chromosome fragments, requiring the presence of either one (i.e., deletion-type aberrations) or two (i.e., exchange-type aberrations) dsb per micronucleus. The detection of additional micronuclei in melanoma cells relative to MC would indicate the presence of excess DNA dsb in melanoma cells. When MC or melanoma cells were assessed for the presence of micronuclei (Fig 6), on an average 0.4%, 28.6%, 26.3%, 2.9%, and 20.6%, respectively, of MC, YUSIT1, YUGEN8, LOX, and YUSAC2 cells contained one or more micronuclei. Expressed as the number of micronuclei observed per 1000 cells, all melanoma cells contained significantly greater numbers of micronuclei than did MC (Table I), with some individual melanoma cells expressing as many as five micronuclei. With the exception of the LOX cells, untreated melanoma cells containing high numbers of γH2AX foci also expressed high numbers of micronuclei. Thus, whereas the correlation between the number of γH2AX foci and the number of micronuclei in melanoma cells is not a direct one, the results are consistent with untreated melanoma cells generally containing greater numbers of micronuclei, and thus DNA dsb, than do MC.

DNA index is higher in melanoma cells A DNA index (DI) was determined by flow cytometry for all melanoma cell lines (Table I). The DI was calculated as the G_1 DNA content of melanoma cells divided by the G_1 DNA content of primary MC. Passage 7 primary human FB were included as an internal standard and had a DI of 1.06 relative to primary MC. All melanoma cells exhibited a DI of between 1.6 and 1.8, consistent with significant increase in ploidy in all the melanoma cell lines examined. Although these results indicated significant changes in the DNA content of the melanoma cells, there was no direct correlation between the DI (aneuploidy) and either the number of γH2AX foci per untreated nucleus or the number of micronuclei per 1000 total cells.

The DNA dsb-induced stress response is defective in melanoma cells Higher basal levels of DNA dsb in melanoma cells might result from a failure of stress-signaling pathways to recognize DNA dsb and articulate this recognition to DNA damage removal processes. To assess this possibility, we examined the integrity of the p53 DNA damage response pathway in MC and melanoma cells. The basal level of p53 protein was similar in untreated MC and YUSAC2 cells, but was significantly elevated, relative to MC, in untreated LOX, YUSIT1, and YUGEN8 cells (Fig 7 and Table II). Using indirect immunofluorescence, we found that the p53 protein in both MC and the YUSAC2 cells was expressed exclusively as a nuclear epitope (results not shown). Elevated basal levels of p53 indicate that the cell's ability to regulate p53 protein levels through transcription or proteolysis is disrupted in LOX, YUSIT1, and YUGEN 8 cells, likely because of mutations in the p53 protein.

The activity of the PIKK-directed, DNA damage response pathway was also assessed. When cells are exposed to IR, the induced DNA dsb are recognized by PIKK such as the ATM protein, which subsequently phosphorylates downstream target proteins (Kastan and Lim, 2000; Bradbury and Jackson, 2003). As the level of IR-induced H2AX histone phosphorylation is the same in all cells examined (Table I), IR-induced activation of the ATM and DNA PK proteins must be intact and equivalent in all five cell types. Another ATM protein target is the Chk2 protein (Chehab *et al*, 2000; Matsuoka *et al*, 2000), which subsequently phosphorylates serine 20 of the p53 protein (Chehab *et al*, 1999; Shieh *et al*, 1999; Hirao *et al*, 2000). Phosphorylation of p53 at serine 20 inhibits hMDM2 ubiquitination of the p53 protein (Shieh *et al*, 1997; Siliciano *et al*, 1997), inhibits p53 degradation by the 26S proteasome (Haupt *et al*, 1997; Kubbutat *et al*,

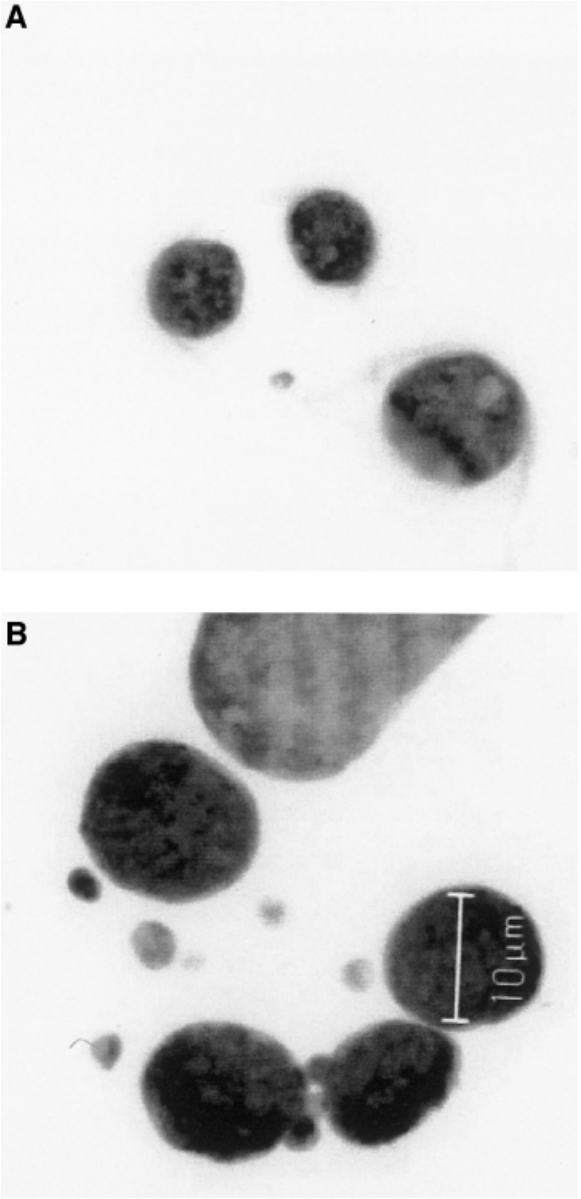

Figure 6
Micronuclei in melanocytes (MC) and YUGEN8 cells. Untreated MC (*Panel A*) or YUGEN8 (*Panel B*) cells were exposed to Cytochalasin B for 48 h as described in Methods. Cells were stained with diamidinophenyl indole (DAPI) and visualized with a fluorescent microscope. Small DAPI stained, extranuclear particles were counted as micronuclei.

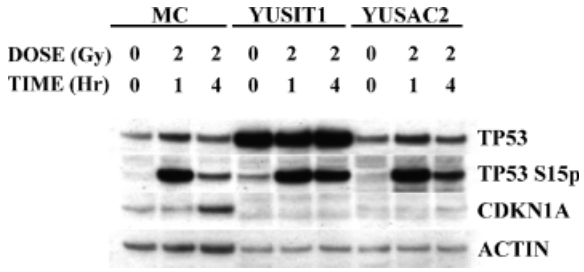

Figure 7
Western analysis of the TP53 DNA damage response pathway in cultured melanocytes (MC) and melanoma cells. MC, YUSAC2, or YUSIT1 cells were exposed to 2 Gy, or left untreated, and replaced at 37°C for 1 or 4 h, as indicated. At these times, cell protein was recovered, separated through PAGE gels, transferred to a membrane, and analyzed by western analysis for the epitopes indicated to the right.

1997), and results in an increase in both the half-life and total cellular content of the p53 protein. IR exposure increased the cellular level of p53 protein in MC, LOX, and YUSAC2 cells (Fig 7 and Table II). Thus, only in MC, LOX, and YUSAC2 cells is the IR-induced pathway intact, resulting in an increase in the half-life of the p53 protein.

Another down-stream target of activated ATM and DNA PK proteins is p53 serine 15 phosphorylation (Banin *et al*, 1998; Canman *et al*, 1998). Phosphorylation of p53 serine 15 plays a role in activation of the p53 protein as a transcription factor (Lambert *et al*, 1998). Relative to the response in MC, p53 serine 15 was phosphorylated significantly only in irradiated YUSIT1 and YUSAC2 cells (Fig 7 and Table II), indicating that although the ATM and DNA PK are functional and activated in all four irradiated melanoma cell lines, they phosphorylate the p53 serine 15 at significant levels only in MC, YUSIT1, and YUSAC2 cells. When p53 is activated as a transcription factor, target genes such as the CDKN1A$^{p21/Waf1}$ gene are transcribed, inducing increases in CDKN1A protein levels. After irradiation, CDKN1A protein levels relative to untreated MC increased significantly only in MC and LOX cells, whereas they declined relative to MC in all other melanoma cell lines (Table II). Thus, the DNA dsb response pathway that is mediated through the p53 protein appears to be intact and fully functional only in primary MC. As the ATM and DNA PK proteins appear to be fully functional, it is likely that this DNA dsb response pathway is disrupted in melanoma cells by mutations in the p53 protein.

Discussion

The transition from MC expressing strict growth control to a proliferating melanoma cell involves a number of biochemical and biological steps (Clark *et al*, 1984; Albino *et al*, 1997). Loss of control of genome stability is generally considered to be a central aspect of any carcinogenesis process (Lengauer *et al*, 1998; Coleman and Tsongalis, 1999). This is the case for melanomagenesis in which melanoma cells express genome instability early on during melanoma development (Albino *et al*, 1997). One type of genome instability that occurs early during melanomagenesis is chromosome instability (Bastian, 2003). Chromosome instability is detectable in mitotic cells as chromosome rearrangements, and is detectable in interphase cells as aneuploidy and/or the presence of micronuclei (Pilch *et al*, 2000; Runger *et al*, 2003).

In this work, we speculated that chromosome instability in melanoma cells results from increases in DNA dsb, and that these dsb would be detected as phosphorylated histone H2AX foci. Structural changes that occur in chromatin surrounding DNA dsb are recognized by the ATM protein (Bakkenist and Kastan, 2003), which phosphorylates the H2AX histone protein in chromatin adjacent to DNA dsb. These high local concentrations of phosphorylated histone H2AX are detected as foci of fluorescence (Rogakou *et al*, 1999; Burma *et al*, 2001; Rothkamm and Lobrich, 2003) (Fig 1). Thus, if chromosome instability in melanoma cells results from high frequencies of DNA dsb, this should be detected as increases in the number of nuclear γH2AX foci. All melanoma cells examined in this report expressed levels of γH2AX foci, as well as chromosome structural and numerical instabilities such as micronuclei and aneuploidy, significantly higher than in primary MC (Table I). We did not,

Table II. Relative level of stress responses in melanoma cells[a]

	Relative p53[b]	p53[c]	p53S15p[d]	CDKN1A[d]
	0 Gy	2 Gy + 1 H	2 Gy + 1 H	2 Gy + 4 H
MC	1.0	4.1	342	8.0
YUSIT1	13.4	0.7	116	0.3
YUGEN8	24.2	0.9	15	0.3
LOX	4.1	1.7	16	3.6
YUSAC2	0.7	3.1	142	0.3

[a]Proliferating melanocytes (MC), YUSIT1, YUGEN 8, LOX, or YUSAC2 melanoma cells were left untreated (Relative p53) or exposed to 2 Gy of γ rays and collected at 1 (p53 or p53s15p) or 4 (CDKN1A) hours. Protein was collected from irradiated or untreated cells, electrophoresed through gels, transferred to membranes and analyzed by western analysis either for the p53 protein (p53), p53 phosphoserine 15 (p53s15p) or CDKN1A protein.
[b]Results are expressed as the ratio of total p53 protein detected in untreated melanoma cells relative to total p53 protein in untreated MC, which is set at 1.0.
[c]Cells were exposed to 2 Gy and collected at 1 h. Results are expressed as the ratio of the total p53 signal detected in treated cells divided by the total signal detected in untreated cells within each cell type.
[d]Cells were exposed to 2 Gy and collected either at 1 (p53 or p53s15p) or 4 h (CDKN1A). Results are expressed as a ratio of the total epitope signal detected in treated cells divided by the total signal detected in untreated MC.Table II results are the average of two repeats.

however, observe a consistent correlation between increased numbers of γH2AX foci and increased numbers of micronuclei in the same untreated melanoma cells (Table I). In fact, the relationship was reversed in two carcinoma cell lines (Table I). Thus, whereas both γH2AX foci and micronuclei are consistently elevated in melanomas, our results are not consistent with there being a direct relationship between the formation of γH2AX foci and the production of micronuclei in untreated melanoma cells.

It remains an interesting question as to why there is such a large increase in the number of γH2AX foci in untreated melanoma cells. Our flow cytometric (FCM) analysis indicates that at least a portion of the increased γH2AX fluorescence in untreated melanoma cells may be explained by an increase, relative to MC cells, in the fraction of melanoma cells that are proliferating. Thus, a portion of the increase in γH2AX foci may be explained by an increase in the proportion of S-phase cells, and thus DNA replication-associated DNA strand breaks, in untreated melanoma cells (Furuta *et al*, 2003). The fraction of melanoma cells in the S phase of the cell cycle is about 2-fold higher than in MC (Table I), and the total γH2AX fluorescence in S- and G_2/M-phase cells is approximately 2-fold greater than that observed in G_1-phase cells (Fig 5). Thus, increased melanoma cell proliferation may explain a portion, but not all, of the increase in γH2AX fluorescence in melanoma cells. As our immunofluorescence procedures detect DNA dsb (Fig 3), the most reasonable explanation for finding higher numbers of γH2AX foci in melanoma cells is that there are higher numbers of DNA dsb in these cells. The presence of increased numbers of DNA dsb in melanoma cells is supported by the co-localization of the γH2AX foci in untreated melanoma cells with DNA dsb-associated proteins such as the ATM, BRCA1, 53BP1, and Nbs1 proteins (Fig 4) and the significant increase in the number of micronuclei that form in these cells (Table I). A molecular explanation for why there would be increases in DNA dsb in melanoma cells is not clear. One obvious possibility is that some environmental agent induces more DNA dsb in the melanoma cells than in MC. As all cells were cultured side by side, this possibility seems unlikely. Another possibility is that a nuclear endonuclease is more active in melanoma cells than in MC. In preliminary experiments in which nuclei from MC or YUSAC2 cells were isolated, placed into an endonuclease friendly buffer and incubated at 37°C for increasing times, nuclear DNA was cut to small fragments faster in YUSAC2 cells than in MC. Thus, YUSAC2 cells may either have more, or more active, nuclear endonucleases than MC; however, because nuclear endonuclease activities are likely under strict control, the involvement of altered nuclear endonuclease activity in the few DNA dsb observed in melanoma cells seems unlikely.

An alternate explanation for the increased numbers of γH2AX foci in melanoma cells might be that histone H2AX adjacent to a nuclear alteration other than a DNA dsb is being recognized by either the ATM or DNA PK proteins in untreated melanoma cells. Consistent with this possibility, we found that the number of γH2AX foci remaining in YUSAC2 cells 12 h after irradiation is the same as the number of foci that existed prior to irradiation (Fig 3). If the DNA changes that result in pre-existing γH2AX foci in YUSAC2 cells were structurally the same as those produced by IR, the DNA dsb repair processes that act of IR-induced dsb should reduce the number of these DNA changes, and thus γH2AX foci, to the level observed in MC 12 h after irradiation. As this did not happen, our results indicate that the repair process involved in rejoining IR-induced dsb is not involved directly in repairing the DNA damage that pre-existed irradiation. Thus, the γH2AX foci pre-existing in untreated melanoma cells must detect DNA alterations that are structurally different from the DNA dsb induced by IR.

Nuclear changes that might have characteristics similar to the ones that produce γH2AX foci in untreated melanoma cells are dysfunctional replication or maintenance of telomeres. Co-localization of a majority of γH2AX foci in untreated melanoma cells with the TRF1 protein suggests that the DNA change being detected by PIKK is associated with telomeres. Telomeres are specialized structures at the ends of linear chromosomes that protect genomic DNA from degradation. Failure to maintain proper telomere length or structure can result in chromosome rearrangements, cell apoptosis, senescence, or permanent inhibition of cell proliferation (Lee *et al*, 1998; Chin *et al*, 1999; Karlseder *et al*, 1999; Smogorzewska and de Lange, 2002). Cancer cells maintain telomere length either by activation of telomerase or by an alternate lengthening of telomeres (ALT) mechanism. Telomeres involved in the ALT replication mechanism co-localize with the BRCA1 protein and the Mre11/Nbs1/Rad50 repair complex (Wu *et al*, 2003). As BRCA1 and Nbs1 proteins co-localize with γH2AX foci in untreated melanoma cells, it is possible that we are detecting telomeres involved in ALT. The majority of melanomas, however, have sufficient telomerase activity to maintain telomere length (Glaessl *et al*, 1999; Parris *et al*, 1999). Thus, it is more likely that the γH2AX foci detected at untreated melanoma cells are at telomeres that are experiencing routine maintenance problems. This speculation is consistent with our observation that the γH2AX foci observed in melanoma cells occur throughout the cell cycle (Fig 5), not primarily during the S phase when telomere replication would be expected. Failure to properly maintain telomere ends can result in uncapped telomeres that activate PIKK such as the ATM protein (Takai *et al*, 2003). Uncapped telomeres are associated with foci of DNA dsb repair proteins such as the phosphorylated ATM and 53BP1 proteins, Mre11 and γH2AX proteins (Takai *et al*, 2003). Consistent with this possibility, we found that a majority of γH2AX foci both in untreated primary and melanoma cells co-localize with the TRF1 protein, as well as with phosphorylated ATM and 53BP1 proteins and the Nbs1 protein (Fig 4). Uncapped telomeres may persist in tumor cells and induce a DNA dsb stress response in cells before and after cells are irradiated. Thus, the γH2AX foci that we observe in untreated melanoma cells may be induced by uncapped telomeres.

Thus, we speculate that the excess γH2AX foci observed in melanoma cells decorate dysfunctional telomeres. In normal cells with functional stress response pathways, uncapped or dysfunctional telomeres are detected by PIKK that signal through stress response pathways such as the p53 DNA damage response pathway, and induce permanent cell growth arrest, senescence or cell death (Lee *et al*,

1998; Chin *et al*, 1999; Karlseder *et al*, 1999; Smogorzewska and de Lange, 2002). Thus, we would expect cells containing aberrant telomeres to be eliminated from the cell population. In primary MC, abnormal telomeres are detected by functional PIKK (Fig 3) that activate functional down-stream stress response pathways such as the p53 pathway (Fig 7). Activation of these stress responses in MC must eliminate cells containing aberrant telomeres as there is no accumulation of γH2AX foci or chromosome damage in normal MC. In contrast, the frequency of γH2AX foci remains high in melanoma cells. Melanoma cells detect DNA damage as efficiently as MC (Fig 3), but cannot launch a fully functional DNA damage stress response (Fig 7). In consequence, cells containing aberrant telomeres are not as effectively eliminated from melanoma populations, ultimately leading to higher levels of chromosome rearrangements such as micronuclei.

A final question is whether the increased DNA strand breaks in melanoma cells lead to chromosome structural instabilities such as increased numbers of micronuclei. Whereas melanoma cells close IR-induced DNA dsb as rapidly and thoroughly as do MC, they do not repair those strand breaks that existed prior to IR exposure (Fig 3). These pre-existing strand breaks apparently persist during mitosis and may lead to the high number of micronuclei observed in binucleate melanoma cells (Table I). Cells from patients with DNA dsb repair recognition and repair disorders, such as ataxia telangiectasia, are known to express high levels of chromosome instability. Failure of PIKK such as the ATM protein to function as DNA dsb sensors is not involved in micronucleus formation in these melanomas because PIKK function normally in MC and all four melanomas, and phosphorylate the H2AX histone in response to IR exposure (Table I). In contrast, stress signaling from the ATM protein sensor through the p53 damage response pathway into activation of the CDKN1A gene is largely nonfunctional in the melanomas (Fig 7 and Table II), presumably because of mutations in the p53 protein. Only in the LOX melanoma does IR induce CDKN1A activation (Table II). Thus, it is possible that the failure of the p53 protein to function either to induce cell cycle blocks or to induce apoptosis, both mechanisms through which cells containing genome damage are removed from the cell population, may be intimately involved in the failure of the melanoma cells to close all DNA dsb.

We conclude that higher numbers of DNA dsb, or chromatin alterations interpreted as DNA strand breaks, are present in interphase melanoma cells than in primary MC. These DNA alterations are detected by PIKK such as the ATM protein, which phosphorylate adjacent H2AX histones producing γH2AX foci. The most likely mechanism for the increased γH2AX foci is that the maintenance or capping of chromosome telomeres is dysfunctional in melanoma cells. Failure to correctly maintain telomeres may result in rearrangements of chromosomal DNA and the production of chromosome rearrangements such as micronuclei.

Materials and Methods

Antibodies A mouse monoclonal antibody against the p53 protein (cat # OP43), a rabbit polyclonal antibody against Nbs1 (cat # PC269), and a mouse monoclonal antibody against BRCA1 (cat # OP92) were purchased from Oncogene (Boston, Massachusetts). A mouse monoclonal antibody against CDKN1A $^{p21/Waf1}$ (cat # sc-817), a goat polyclonal antibody against human actin (cat # sc-1616) and a goat polyclonal antibody against TRF1 protein (cat # sc-1977) were purchased from Santa Cruz Biotechnology (Santa Cruz, California). A mouse monoclonal antibody (cat # 05–636) and a rabbit polyclonal antibody (cat # 07–164) against H2AX histone phosphorylated on serine 139 (γH2AX) were purchased from Upstate Biotechnology (Charlottesville, Virginia). A rabbit polyclonal antibody against TP53 phosphoserine 15 (cat # 9284) was purchased from Cell Signaling Technology (Beverly, Massachusetts). A rabbit polyclonal antibody against 53BP1 protein was provided by Dr Phillip B. Carpenter, Department of Biochemistry and Molecular Biology, University of Texas Health Sciences Center, Houston, Texas. A mouse monoclonal antibody against ATM phosphoserine 1981 (cat # 200–301–400) was purchased from Rockland Immunochemicals (Bilbertsville, Pennsylvania).

Tissue collection, preparation of primary skin cells, and cell treatment Discarded human neonatal foreskins were collected in accordance with the University of Utah's Institutional Review Board Policies from the LDS Hospital in Salt Lake City, Utah (IRB#9476–01). The tissue was collected at room temperature in 1X Ham's F12 medium (Gibco, Carlsbad, California) supplemented with antibiotic–antimycotic solution (Gibco-BRL 15240–039). The skin was trimmed of excess fat and connective tissue, rinsed several times with phosphate-buffered saline (PBS), and dissected into approximately 3.5 mm^2 sections. Primary cells were isolated from these skin sections as described elsewhere (Bowen *et al*, 2003). Neonatal human MC were cultured in Hams F12 medium supplemented with 7.5% calf serum, 1% glutamine, 100 μM 3-isobutyl-1-methylxanthine, 200 μg per L cholera toxin, 1 μM sodium orthovanadate, and 0.08 μM phorbol 12-myristate 13-acetate. MC were cultured at 37°C in a 5% CO_2 environment and were used between passages 1 and 5. All melanoma cell lines and HaCaT cells were obtained from Dr D. Grossman (University of Utah, Huntsman Cancer Institute, Salt Lake City, Utah). HeLa cells were obtained from the American Type Culture Collection. All cancer cell lines were cultured in F12 medium supplemented with 10% fetal bovine serum (FBS). All melanoma cell lines are from metastatic melanomas. The LOX cell line (Fodstad *et al*, 1988) is from an amelanotic axilliary lymph-node metastasis that developed in a 58-y-old Caucasian male, the YUGEN8 is from the left frontal brain, and the YUSAC2 is from the left neck, whereas the exact metastatic location of the YUSIT1 melanoma is unknown (Dr R. Halaban, personal communication). HeLa cells were originally isolated from a cervical adenocarcinoma and the HaCaT cells from a cutaneous squamous cell carcinoma. Cells were irradiated in whole medium with γ rays using the Shephard Mark I ^{137}Cs Irradiator (J. L. Shepherd & Associates, San Fernando, California) at a dose rate of 4.7 Gy per min at the Huntsman Cancer Institute's Irradiation Facility. Cells were replaced into a 37°C incubator immediately after irradiation and collected at appropriate post-treatment times, as indicated.

FCM analyses FCM analysis of DNA distributions was performed with a Facscan 1 Flow Cytometer (Becton Dickenson, San Jose, California) on cells that had been fixed in 70% ethanol, as previously described (Warters, 1992). Flow cytometry results were analyzed with ModFit 1 software. The DI was calculated as the ratio of the G_1 DNA content in cancer cells over the G_1 DNA content of MC. Flow cytometry analysis of γH2AX expression throughout the cell cycle was performed as previously described (MacPhail *et al*, 2003). In brief, cells previously fixed with 70% ethanol were rehydrated in Tris-buffered saline (TBS) containing 4% FBS and 0.1% Triton × 100, exposed to a 1/500 dilution of a monoclonal antibody against γH2AX, washed free of primary antibody, exposed to a 1/200 dilution of an Alexa 488-conjugated, anti-mouse secondary antibody, washed free of secondary

antibody, stained with propidium iodide, and analyzed with the Facscan 1 Flow Cytometer for both the amount of DNA and γH2AX fluorescence signal per cell. A negative control group (i.e., cells exposed to a nonspecific mouse immunoglobulin G_1) was run alongside each anti-γH2AX monoclonal antibody exposed group.

Immunofluorescence microscopy Cells were plated onto 35 mm^2 plastic dishes. Cells were washed with PBS and fixed either with 2% paraformaldehyde in PBS for 7 min or with 100% methanol for 10 min at −20°C. The cells were rinsed to remove fixative, permeabilized with Triton X-100, and rinsed with PBS. The cells were exposed to a blocking solution of either 0.1% bovine serum albumin (BSA) (for monoclonal γH2AX and 53BP1), 10% calf serum (for Nbs1 and BRCA1), or 5% donkey serum (for TRF1). Primary antibody was diluted (1:500 for γH2AX, 1:300 for 53BP1, 1:150 for BRCA1, and 1:100 for polyclonal γH2AX, Nbs1 and TRF1) in either PBS or 0.1% BSA in PBS and exposed to the cells for 1 h at room temperature or for 30 min at 37°C for 53BP1. Cells were rinsed with PBS for 5 min, three times before being exposed to Alexa 488 and/or Alexa 568 (Molecular Probes, Eugene, Oregon)-conjugated anti-mouse, anti-goat, or anti-rabbit secondary antibody. The cells were exposed to 0.7 μM diamidinophenyl indole (DAPI), a nuclear DNA stain. The cells were washed three times with PBS for 5 min each and mounted with Fluorsave (Calbiochem, La Jolla, California) antifade mounting solution. Cells were visualized using an Olympus Provus microscope (Olympus America Inc., Melville, New York) using a 100 × objective. Images were captured using Axiovision software. Forty to 150 cells were counted per point.

Micronucleus assay Quantification of micronuclei was performed similar to previous reports (Fenech and Morley, 1986; Gutierrez-Enriquez and Hall, 2003). Cells were cultured on 35 mm^2 dishes, incubated in 3 μg per mL Cytochalasin B for 48 h, rinsed with PBS, fixed with 100% methanol at −20°C, and air-dried. Cells were rehydrolyzed with PBS, stained with 0.7 μM DAPI, mounted onto slides with Fluorsave, allowed to dry, and then stored at −20°C until counted. Micronuclei were counted if they had roughly the same fluorescence intensity as nuclei and were clearly distinguishable as nonnuclear particles. Binucleated cells were defined using the bright field, white light. At least 1000 binucleated cells were counted on an Olympus Provus microscope using a × 60 objective. Approximately 40% of MC and 60% of melanoma cells were observed as binucleated cells after 48 h of Cytochalasin B treatment.

Cell protein analysis by western blotting Cell protein was recovered by scraping cells into a RIPA buffer (50 mM Hepes, 150 mM NaCl, 5 mM EDTA, 1 mM EGTA, 1 mM NaF, 15 mM *p*-nitrophenyl phosphate, disodium hexahydrate, 2 mM $NaVO_4$, 1 mM DTT, 2 mM PMSF, 1% NP-40, 0.1% SDS, 1% Triton X-100, 1% deoxycholate, and a 1:400 dilution of a Protease inhibitor cocktail) (Sigma cat# P1860, St. Louis, Missouri)). Protein content was determined using a Bradford colorimetric reaction (BioRad, Hercules, California). Protein samples were electrophoresed through SDS, 4%–12% polyacrylamide gradient gels (InVitrogen, Carlsbad, California) in 2-(N-morpholino) ethane sulfonic acid/Tris-SDS running buffers at 150 V, and electrotransferred onto a polyvinylidene fluoride (PVDF) membrane at 220 mA at 4°C. Protein epitopes transferred to the PVDF membranes were detected using primary antibodies dissolved in TBS containing 0.1% Tween 20 and 5% non-fat dried milk. Primary antibodies were identified using a horseradish peroxidase-labeled secondary antibody and by exposure to Amersham Hyperfilm ECL photographic film using Amersham ECL (or ECL Plus) (Amersham Biosciences, Piscataway, New Jersey) chemiluminescence reagents according to the manufacturer's recommendations. Exposed films were quantified using a BioRad Model GS-700 Imaging Densitometer. Density units for each photographic negative band were corrected for variations in loading using the actin band as the reference and normalized against the unirradiated control lane.

The authors thank the Cell Culture Core facility of Yale Skin Diseases Research Center (supported by USPH grant AR41942, R.E. Tigelaar Program Investigator) for providing the melanoma cell lines used in this report. We would also like to thank the Huntsman Cancer Institute for the use of the fluorescence microscope and the irradiation facility. We thank Dr Wayne Green, Director of the Health Sciences Center Flow Cytometry Facility, for his help in analysis of flow cytometry results. This research was supported by the Office of Science (BER), US Department of Energy, Grant number DE-FG03-01ER63240.

DOI: 10.1111/j.0022-202X.2005.23674.x

Manuscript received November 16, 2003; revised May 27, 2004; accepted for publication July 26, 2004

Address correspondence to: Dr Raymond L. Warters, Department of Radiation Oncology, University of Utah Health Sciences Center, Salt Lake City, Utah 85132, USA. Email: ray.warters@hsc.utah.edu

References

Albino A, Reed J, McNutt N: Molecular biology of cutaneous melanoma. In: DeVita VT, Hellman S, Rosenberg SA (eds). Cancer: Principles and Practice of Oncology, 5th edn. Philadelphia, Pennsylvania: Lippincott, 1997; p 1935–1946

Bakkenist CJ, Kastan MB: DNA damage activates ATM through intermolecular autophosphorylation and dimer dissociation. Nature 421:499–506, 2003

Banin S, Moyal L, Shieh SY, *et al*: Enhanced phosphorylation of p53 by ATM in response to DNA damage. Science 281:1674–1677, 1998

Bastian BC: Understanding the progression of melanocyte neoplasia using genomic analysis: From fields to cancer. Oncogene 22:3081–3086, 2003

Bowen AR, Hanks AN, Allen SM, Alexander A, Diedrich MJ, Grossman D: Apoptosis regulators and responses in human melanocytic and keratinocytic cells. J Invest Dermatol 120:48–55, 2003

Bradbury JM, Jackson SP: The complex matter of DNA double-strand break detection. Biochem Soc Trans 31:40–44, 2003

Burma S, Chen BP, Murphy M, Kurimasa A, Chen DJ: ATM phosphorylates histone H2AX in response to DNA double-strand breaks. J Biol Chem 276:42462–42467, 2001

Canman CE, Lim DS, Cimprich KA, *et al*: Activation of the ATM kinase by ionizing radiation and phosphorylation of p53. Science 281:1677–1679, 1998

Celeste A, Fernandez-Capetillo O, Kruhlak MJ, *et al*: Histone H2AX phosphorylation is dispensible for the initial recognition of DNA breaks. Nature Cell Biol 5:675–679, 2003

Chehab NH, Malikzay A, Appel M, Halazonetis TD: Chk2/hCds1 functions as a DNA damage checkpoint in G1 by stabilizing p53. Genes Dev 14: 278–288, 2000

Chehab NH, Malikzay A, Stavridi ES, Halazonetis TD: Phosphorylation of Ser-20 mediates stabilization of human p53 in response to DNA damage. Proc Natl Acad Sci USA 96:13777–13782, 1999

Chin L, Artandi SE, Shen Q, *et al*: P53 deficiency rescues the adverse effects of telomere loss and cooperates with telomere dysfunction to accelerate carcinogenesis. Cell 97:527–538, 1999

Chong L, van Steensel B, Broccoli D, Erdjument-Bromage H, Hanish J, Tempst P, de Lange T: A human telomeric protein. Science 270:1663–1667, 1995

Clark WH, Elder DE, Guerry D, Epstein MN, Greene MH, van Horn M: A study of tumor progression: The precursor lesions of superficial spreading and nodular melanoma. Hum Pathol 15:1147–1165, 1984

Coleman WB, Tsongalis GJ: The role of genomic instability in human carcinogenesis. Anticancer Res 19:4645–4664, 1999

Fagagna FD, Reaper PM, Clay-Farrace L, *et al*: A DNA damage checkpoint response in telomere-initiated senescence. Nature 426:194–198, 2003

Fenech M, Morley AA: Cytokinesis-block micronucleus method in lymphocytes: Effect of *in vivo* ageing and low dose X-irradiation. Mutat Res 161: 193–198, 1986

Fodstad O, Aamdal S, McMenamin M, Nesland JM, Pihl A: A new experimental metastasis model in athymic nude mice. The human malignant melanoma LOX. Int J Cancer 41:442–449, 1988

Furuta T, Takemura H, Liao Z, *et al*: Phosphorylation of histone H2AX and activation of Mre11, Rad50, and Nbs1 in response to replication-dependent DNA double-strand breaks induced by mammalian DNA Topoisomerase I cleavage complexes. J Biol Chem 278:20303–20312, 2003

Glaessl A, Bosserhoff AK, Buettner R, Hohenleutner U, Landthaler M, Stolz W: Increase in telomerase activity during progression of melanocytic cells

from melanocytic naevi to malignant melanomas. Arch Dermatol Res 291:81–87, 1999

Gutierrez-Enriquez S, Hall J: Use of the cytokinesis-block micronucleus assay to measure radiation-induced chromosome damage in lymphoblastoid cell lines. Mutat Res 535:1–13, 2003

Haupt Y, Maya R, Kazaz A, Oren M: Mdm2 promotes the rapid degradation of p53. Nature 387:296–299, 1997

Hirao A, Kong Y, Matsuoka S, *et al*: DNA damage-induced activation of p53 by the checkpoint kinase Chk2. Science 287:1824–1827, 2000

Hussein MRA, Wood GS: Molecular aspects of melanocyte dysplastic nevi. J Molec Methods 4:71–80, 2002

Jhappan C, Noonan FP, Merlino G: Ultraviolet radiation and cutaneous malignant melanoma. Oncogene 22:3099–3112, 2003

Karlseder J, Broccoli D, Dai Y, Hardy S, De Lange T: p53-and ATM-dependent apoptosis induced by telomeres lacking TRF2. Science 283:1321–1325, 1999

Kastan MB, Lim DS: The many substrates and functions of ATM. Nat Rev Mol Cell Biol 1:179–186, 2000

Kubbutat MHG, Jones SN, Vousden KH: Regulation of p53 stability by mdm2. Nature 387:299–303, 1997

Lambert PK, Kashanchi F, Radonovich MF, Shiekhatter R, Brady JN: Phosphorylation of p53 serine 15 increases interaction with CBP. J Biol Chem 273:33048–33053, 1998

Lee HW, Blasco MA, Gottlieb GJ, Horner JW, Greider CW, DePinho RA: Essential role of mouse telomerase in highly proliferative organs. Nature 392: 569–574, 1998

Lengauer C, Kinzler KW, Vogelstein B: Genetic instabilities in human cancers. Nature 396:643–649, 1998

MacPhail SH, Banath JP, Yu Y, Chu E, Olive PL: Cell cycle dependent expression of phosphorylated histone H2AX: Reduced expression in unirradiated but not X-irradiated G1-phase cells. Radiat Res 159:759–767, 2003

Matsuoka S, Rotman G, Ogawa A, Shiloh Y, Tamai K, Elledge SJ: Ataxia telangiectasia-mutated phosphorylates Chk2 *in vivo* and *in vitro*. Proc Natl Acad Sci USA 97:10389–10394, 2000

Mirzoeva OK, Petrini JHJ: DNA replication-dependent nuclear dynamics of the Mre11 complex. Molec Cancer Res 1:207–218, 2003

Park EJ, Chan DW, Park JH, Oettinger MA, Kwon J: DNA-PK is activated by nucleosomes and phosphorylates H2AX within the nucleosomes in an acetylation-dependent manner. Nucleic Acids Res 31:6819–6827, 2003

Parris CN, Jessard S, Silver A, MacKie R, McGregor JM, Newbold RF: Telomerase activity in melanoma and non-melanoma skin cancer. Br J Cancer 79:47–53, 1999

Petrini JHJ, Stracker TH: The cellular response to DNA double-strand breaks: Defining the sensors and mediators. Trends Cell Biol 13:458–462, 2003

Pilch H, Gunzel S, Schaffer U, Tanner B, Heine M: Evaluation of DNA ploidy and degree of DNA abnormality in benign and malignant melanocytic lesions of the skin using video imaging. Cancer 88:1370–1377, 2000

Rogakou EP, Boon C, Redon C, Bonner WM: Megabase chromatin domains involved in DNA double-strand breaks *in vivo*. J Cell Biol 146:905–915, 1999

Rogakou EP, Nieves-Neira W, Boon C, Pommier Y, Bonner WM: Initiation of DNA fragmentation during apoptosis induces phosphorylation of H2AX histone at serine 139. J Biol Chem 31:9390–9395, 2000

Rogakou EP, Pilch DR, Orr AH, Ivanova VS, Bonner WM: DNA double-strand breaks induced histone H2AX phosphorylation on serine 139. J Biol Chem 273:5858–5868, 1998

Rothkamm K, Lobrich M: Evidence for a lack of DNA double-strand break repair in human cells exposed to very low x-ray doses. Proc Natl Acad Sci USA 100:5057–5062, 2003

Runger TM, Kotas M, Poot M, Leverkus M, Epe B, Jeggo PA, Hellfritsch D: Reduced joining of DNA ends correlates with chromosomal instability in three melanoma cell lines. Tumor Biol 24:100–108, 2003

Sedelnikova OA, Rogakou EP, Panyutin IG, Bonner WM: Quantitative detection of 125IdU-induced DNA double strand breaks with γ-H2AX. Radiat Res 158:486–492, 2002

Shen M, Haggblom C, Vogt M, Hunter T, Lu KP: Chracterization and cell cycle regulation of the related human telomeric proteins Pin2 and TRF1 suggest a role in mitosis. Proc Natl Acad Sci USA 94:13618–13623, 1997

Shieh S, Ikeda M, Taya Y, Prives C: DNA damage-induced phosphorylation of p53 alleviates inhibition by Mdm2. Cell 91:325–334, 1997

Shieh S, Taya Y, Prives C: DNA damage-inducible phosphorylation of p53 and N-terminal sites including a novel site, Ser20, requires tetramerization. EMBO J 18:1815–1823, 1999

Siliciano JD, Canman CE, Taya Y, Sakguchi E, Appella E, Kastan MB: DNA damage induces phosphorylation of the amino terminus of p53. Genes Dev 11:3471–3481, 1997

Smogorzewska A, de Lange T: Different telomere damage signaling pathways in human and mouse cells. EMBO J 21:4338–4348, 2002

Stiff T, O'Driscoll M, Rief N, Iwabuchi K, Lobrich M, Jeggo PA: ATM and DNA-PK function redundantly to phosphorylate H2AX after exposure to ionizing radiation. Canc Res 64:2390–2396, 2004

Takai H, Smorgorzewska A, de Lange T: DNA damage foci at dysfunctional telomeres. Curr Biol 13:1549–1556, 2003

Warters RL: Radiation-induced apoptosis in a murine T cell hybridoma. Cancer Res 52:883–890, 1992

Warters RL, Lyons BW: Variation in radiation-induced formation of DNA double strand breaks as a function of chromatin structure. Radiat Res 130:309–318, 1992

Wu G, Jiang X, Lee W, Chen P: Assembly of functional ALT-associated promyelocytic leukemia bodies requires Nijmegen Breakage Syndrome 1. Cancer Res 63:2589–2595, 2003

Wyllie AH, Kerr JFR, Currie AR: Cell death: The significance of apoptosis. Int Rev Cytol 68:251–306, 1980